Seismic Performance of Base Isolated Nuclear Power Plants under Real & Simulated Long-Period Seismic Excitations

Ahmer Ali & Dookie Kim
Department of Civil Engineering, Kunsan National University, Republic of Korea

Yinfeng Dong
College of Civil Engineering, Chongqing University, Chongqing, China

Sung Gook Cho
R &D Center, JACE KOREA Company, Gyeonggi-do, Republic of Korea

SUMMARY:
The abundance of the earthquake events in the past has necessitated the use of seismic isolation devices for safety related structures. The ongoing research trend is mainly dealt with the improvisations and enhancing the sustainability of the base isolated nuclear power plants (NPPs). The present study focuses on evaluating the performance of base isolated NPPs subjected to real and simulated long-period seismic excitations. The ground motions are selected according to the performance based regulatory guide for the safety related structures issued by U.S Nuclear Regulatory Commission (NRC). A simplified ARMA model approach is used to generate the ground motions. A set of seven seismic motions recorded during Tohoku earthquake with the high long-period component are applied to the base isolated NPP model. The obtained responses are compared with those resulted from ground motions of common nature. The results are discussed with the suggestions for the future research and provisions in the seismic code.

Keywords: Seismic response, Long-period motions, Generation, ARMA model, Nuclear power plant

1. INTRODUCTION

Recently, the issue of long-period ground motions is gaining importance because of the rapidly growing large-scale structures like high-rise buildings, sky scrapers, oil storage tanks and long span bridges. The medium and long-period structures such as base isolated buildings can also be affected by the long-period component of the far-source or near-fault seismic excitations. In this context, the devastating hit of Tohoku earthquake occurred off the pacific coast of Japan on March 11, 2011 has caused extreme disasters due to high tsunami waves and strong ground motions. As, the subduction zone earthquakes like Tohoku produce long-period, long-duration ground motions at larger distance from the rupture zone that tend the long-period structures to resonate for longer durations and can credibly lead to severe structural damages and stability hazards. In this regard, the uncertainty of such ground motions and their effect on structural behavior has been taken as an important issue. Therefore, the stochastic approach for the simulation of acceleration records for the hazard evaluation and structural response has been practiced for years. Limited studies have been carried out on the categorization and generation of the long-period character of a seismic input and the dynamic characteristics of medium and long-period structures subjected to such strong ground motions.

Tkewaki (2011) and Tkewaki *et al.* (2011) reported the severe aspects of the devastating Tohoku earthquake along with the response characteristics of the tall buildings under the resonance and critical impact of the recorded long-period motions. The observed velocity and earthquake input energy spectra strongly inferred the presence of fairly large long-period wave components in the Tohoku records. The buildings were noticed to efficiently damp the corresponding vibrations using high-hardness rubber dampers, in shorter durations comparative to the buildings without dampers. Xiang and Li (2000) analyzed the characteristics of long-period response spectra of strong ground motions recorded in US. The horizontal motion components were grouped in terms of site categorization and corner periods of the spectra were statistically determined corresponding to the design spectrum of

China. The long-period spectra presented in this study were suggested to be referred for the revision of the seismic design code of buildings in China. Araki *et al.* (2011) examined the dynamic instability in high-rise steel moment resisting frames subjected to a pair of strong long-period ground motions. The drifting trend was found quite prominent in the lower stories when the natural periods of the high-rise steel frame were close to the dominant periods of the seismic inputs. Moreover, the drifting either led to residual inter story drift ratio over 0.01, or to collapse corresponding to the smaller design base shear. Hurtado *et al.* (1996) reported the stochastic response of isolated buildings subjected to strong bidirectional seismic inputs. The work is mainly focused on the effects of the response of non-stationary character of the seismic excitation and the upshots of the biaxial loading. A sequence of low frequency cycles in the excitation has reflected its non-stationary nature and caused a credible increase in the displacements of the isolation device and the superstructure.

Some studies have been reported on the simulation and generation of earthquake records also. Dong *et al.* (2004) proposed the method based on time varying vector ARMA model to simulate a set of ground motions in the time and frequency domain. In this study, Kalman filter was applied to estimate the time varying parameters of ARMA model. The method has shown nice agreement between the actual and simulated ground motions. Mobarakeh *et al.* (2002) used a simplified time invariant ARMA (2, 1) model to successfully generate earthquake motions by reproducing the non-stationary amplitude as well as the frequency content of the acceleration record. Popescu and Demetriu (1990) presented a method to analyze and simulate the strong earthquake motions using parametric ARMA models. The results were found promising and suggested to be utilized in the design of engineering structures.

In this study, the performance and the probabilistic response of the base isolated nuclear power plants (NPPs) subjected to strong real and simulated seismic motions have been numerically investigated using OpenSees platform. The earthquake inputs with fairly large long-period component and, of common nature are selected corresponding to the guidelines provided by the performance based regulatory guide for the safety related structures issued by U.S Nuclear Regulatory Commission (NRC) relevant to spectral compatibility. The ground motions are then generated using ARMA model approach. The dense recordings are obtained through the K-NET and KiK-net strong ground motion networks for Tohoku mega thrust earthquake. The comparative response of the base-isolated NPP under long-period and common earthquake inputs is taken under discussion to demonstrate the substantially significant impact of long-period ground motions.

2. SELECTION & GENERATION OF GROUND MOTIONS

2.1. SELECTION

Tohoku earthquake is primarily considered because of its lengthy time history and better demonstration of the long-period component in the recorded spectra. Eventually, seismic motions of common nature were also recorded and so adopted from this event. In earthquake response analysis, the theory of response spectra is fundamentally involved where it further contributes to the design based methods for most of the seismic codes used worldwide. So, the input data for two groups of motions i.e. long and short-period; are selected based on the target spectrum specified by the NRC performance based regulatory guide.

Dual frequency band method proposed by Yang *et.al* (2000) is adopted to select the inputting waves for the time history analyses. The method is designated to control the relative errors in two frequency domains, which are corresponding to the flat range of the target response spectrum as well as the natural period of the structure as shown in Figure 1. According to ASCE-7/10 16.1.3.1, the ground motions should be scaled such that the average value of the 5 percent damped response spectra for the suite of motions is not less than the designed response spectrum for the site for periods ranging from 0.2 T to 1.5 T. Here, T refers to the natural period of the structure in the fundamental mode for the direction of response being analyzed.

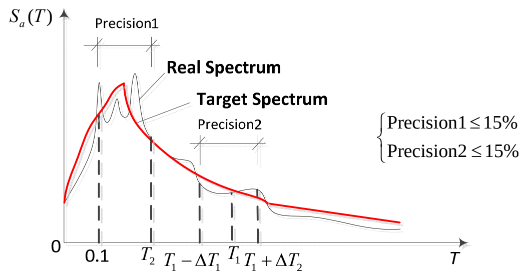

$$\text{Precision1} = \left| \frac{S_a(T_i) - S_a^T(T_i)}{S_a^T(T_i)} \right| \Big/ N_1 \qquad 0.1 \le T_i \le T_2,\ i = 1, 2, \cdots N_1$$

$$T_2 = 0.75$$

$$\text{Precision2} = \left| \frac{S_a(T_i) - S_a^T(T_i)}{S_a^T(T_i)} \right| \Big/ N_2 \qquad T_1 - \Delta T_1 \le T_i \le T_1 + \Delta T_2,\ i = 1, 2, \cdots N_2$$

$$T_1 - \Delta T_1 = 1.1$$

$$T_1 + \Delta T_2 = 2.2$$

Figure 1. Criteria for selecting input waves for time history analyses.

2.2. GENERATION

Seven ground motions for each long and short-period earthquakes are generated. A simplified ARMA model approach based on time-variant ARMA parameters used by Dong (2000) is used to simulate the seismic motions of common nature followed by the process shown in Figure 2(a). The process initiates by specifying the model order; satisfying the AIC (Akaike Information Criterion) criterion for the estimated model. Smaller value of AIC indicates a better model. The coefficients of ARMA model are then estimated along with the data residual using kalman filter. The normally distributed white noise w_n is generated which should be concurrent with the statistical distribution of the residual e_i. The acceleration data is synthesized using the estimated ARMA coefficients and white noise to get the simulated earthquake time history. The spectral compatibility of the real and generated ground motions is made sure by comparing the relative error e_{rr} with the threshold error e_t. If the precision is found out of the range of 10~15 %, the process is required to be repeated followed by the regeneration of white noise w_n , until the desired precision is not achieved. For multiple generation of ground motions, the input of multiple estimation of white noise is required as shown in Figure 2(a).

The long-period ground motions are simulated followed by the chart; shown in Figure 2(b). The motion data is decomposed by using wavelet transform to acquire the separate time history of high and low frequency content of the particular earthquake. Later, the high frequency component is simulated by using the above stated ARMA model scenario. The respective output is then adjoined with the low frequency content to get the final form of generated earthquake. The precision of 10~15% is made sure to check the spectral compatibility of the real and simulated ground motions.

Figure 3(a,b) demonstrates the successful application of the above stated processes by comparing the response spectra of a simulated long and short-period ground motions with that of real ground motions, respectively. The desired concurrence is fairly achieved. Moreover, Figure 3(c) signifies the mean spectrum of the two groups of real and simulated ground motions in comparison with the design spectrum. The maximum deviation in the mean spectra is noticed in the period range of 0.5 to 1.0 sec approx. The natural period 1.345 sec, of the base isolated NPP and the corresponding average spectral acceleration of the mean long and short-period earthquake is clearly pointed in the figure. Beyond 1.345 sec, the spectra seem to go along the designed one whereas the major magnitude difference can be clearly seen before the specified time period.

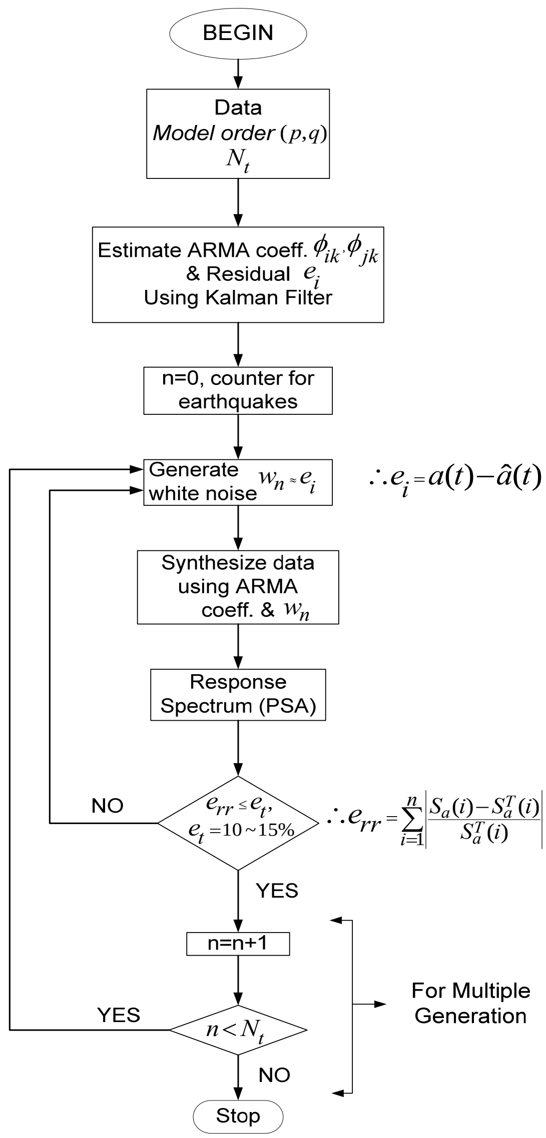

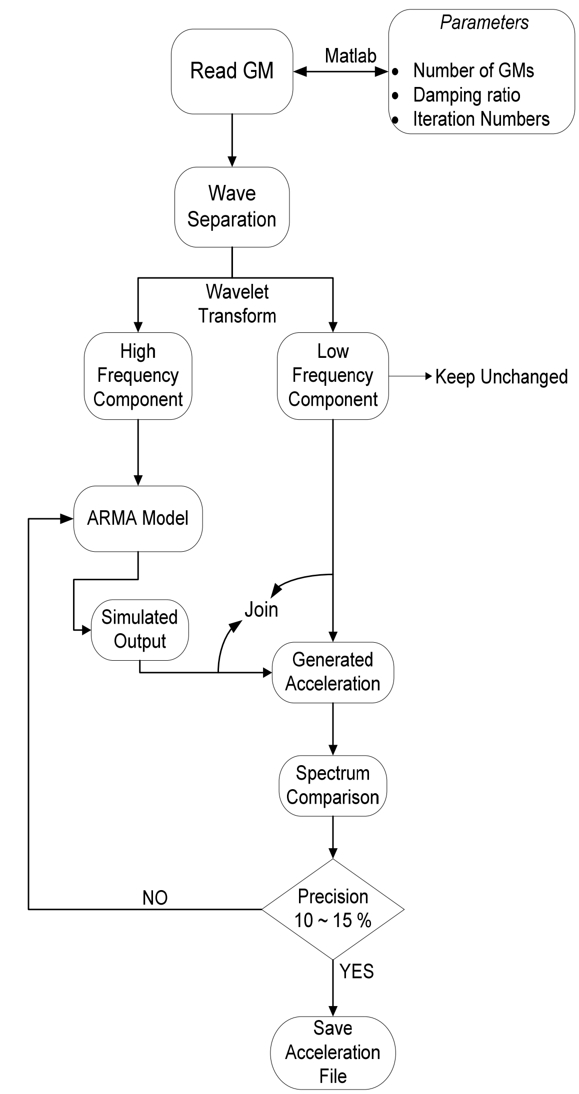

Figure 2(a). Flow Chart for ARMA simulation of short-period ground motions

Figure 2(b). Flow Chart for simulation of long-period ground motions

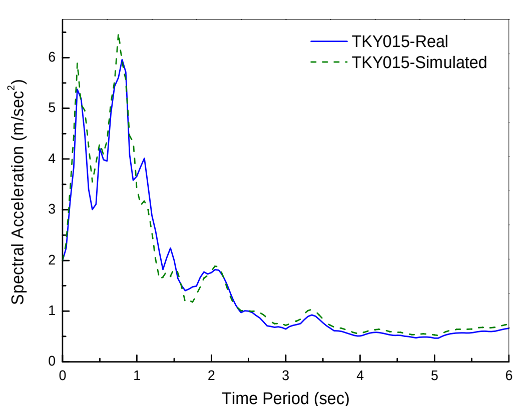

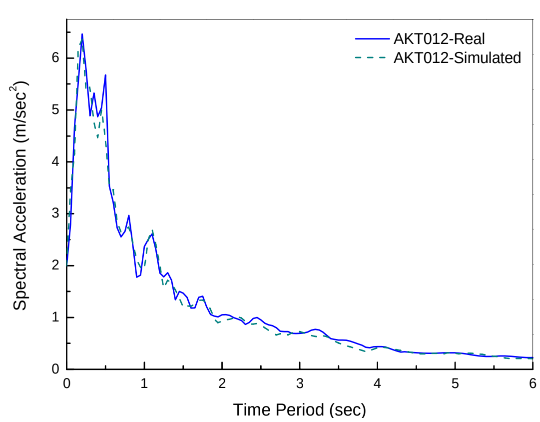

Figure 3(a). Comparative acceleration response spectra of real & simulated long-period ground motion

Figure 3(b). Comparative acceleration response spectra of real & simulated short-period ground motion

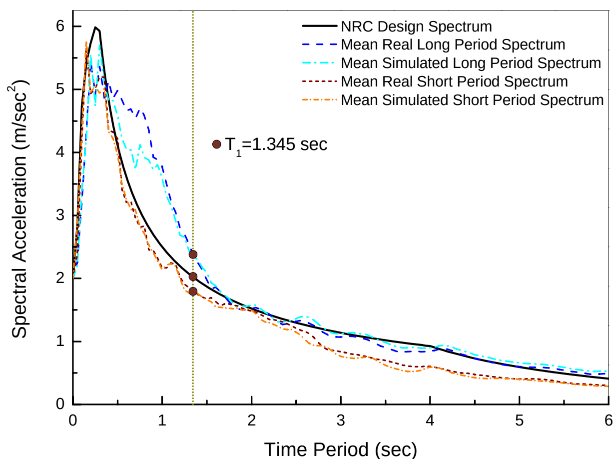

Figure 3(c). Comparison of mean long and short-period spectra with the NRC design spectrum

3. THE NPP MODEL

The structural stick model of the NPP reactor building (Lee and Song, 1999) was modeled in the OpenSees platform (McKenna and Fenves, 2001). The finite element model is 65.84 m long and contains 15 nodes and 14 elements, where the first element initiating from the base comprises a highly stiff zero-length elastomeric bearing element as shown in Figure 4. The actual masses are transferred as lumped to the corresponding nodes of each element. The average translational mass associated to each node is 2221 $KN.s^2/m$ where the mean area and moment of inertia of each element is 168.69 m^2 and 39803.40 m^4. The allowable displacement of the bilinear isolator is calculated using guidelines provided by Naeim and Kelly (1999). The simulated inputs were applied at the base of the NPP model with the PGA 0.2g. The response was recorded in terms of shear force, displacement and the hysteresis energy. Whereas the response of NPP subjected to real long and short-period ground motions was adopted from the study previously done by the authors (Ali *et.al* 2012). Hence, the probabilistic mean of the responses were used for the significant comparison of the structure for both type of earthquakes.

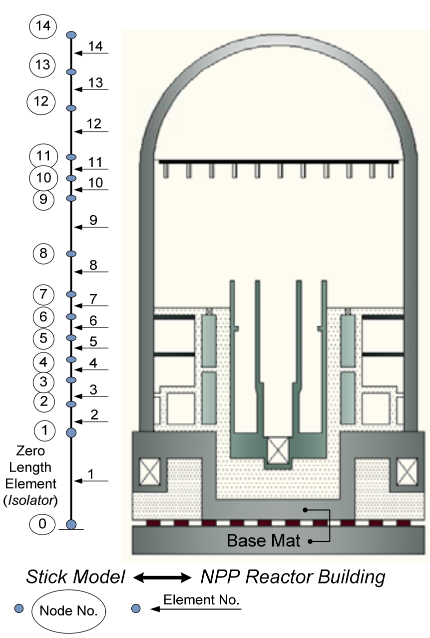

Figure 4. NPP reactor building and Stick Model

4. RESULTS & DISCUSSIONS

The dynamic numerical analyses give the comprehensive picture of the performance of the NPP in terms of maximum displacement, attributed shear force at each node, the cyclic and the overall energy dissipated by the structure.

Figure 5(a) shows the mean nodal displacements of isolated NPP under real and simulated long and short-period earthquakes. It can be observed that in each case the isolator displacement is quite large and predominant such that the relative displacement of the superstructure is small which in turn can be neglected. In case of real long-period motion inputs, the mean maximum displacement attained by the isolator is 0.1246 m which is fairly large compared to that of real short-period motions i.e. 0.0875 m. Similarly, for simulated long-period ground motions, the mean displacement is 0.12063 m; higher than that of the value acquired by short-period simulated motions i.e. 0.0898 m. Therefore, the deviating percentile almost approaches 30% and 26% for both types of real and simulated motion inputs, respectively. The probabilistic displacement values presented in table 1 seem to exceed the allowed displacement of 0.157 m but the limit is not crossed in case of common natured ground motions. The evident generation and propagation of the long-period wave component, specifically from a far-source earthquake is distinctly elaborated in most of the seismic provisions. In addition, the scenario can turn cumbrous if the structure is located over deep soil plateau and in high seismic hazard area. Consequently, the long-period ground motion of even moderate intensity may cause failure of NPP.

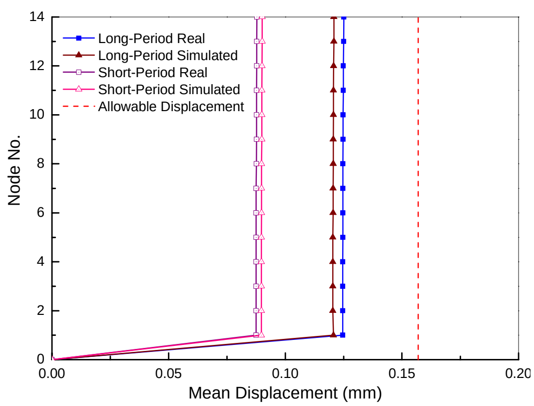

Figure 5(a). Comparison between mean nodal displacement (mm)

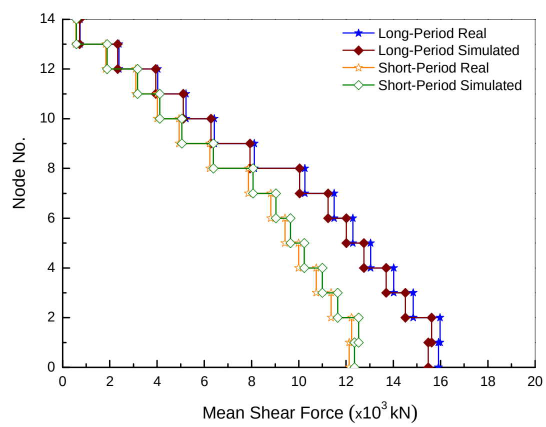

Figure 5(b). Comparison between mean shear force (x10^{3}kN)

The mean shear forces along the NPP are shown in Figure 5(b). For the each type of ground motions it can be seen that the maximum resistance is shown by the base followed by a couple of nodes from the bottom. The shear forces after the first two elements have shown a gradual descending trend which approaches to minimum at the top node. Moreover, the higher effect of long-period components for both real and simulated motions, is credibly reflected as the response is fairly amplified in this case due to greater intensity when compared to the short-period excitations.

For the clear demonstration, the comparative probabilistic values of the shear force for both long and short-period ground motions are illustrated in Table 1. The mean shear force at the base node due to real long-period motion input can be visualized as 24% larger than real short-period motions. Whereas, for simulated excitations the difference is almost 20.1%. Moreover, the change in the difference of forces with the height is quite clear in Figure 5(b). A large deviation can be observed initially but it lessens up gradually with the elevation and the difference turned negligibly small at the end nodes.

Table 1. Mean displacement & shear force response comparison at base isolated node for long & short-period earthquakes

	Long-Period Earthquake Input		Short-Period Earthquake Input	
	Real	Simulated	Real	Simulated
Mean Displacement (m)	0.1246	0.12063	0.0875	0.0898
Standard Deviation σ_D	0.0377	0.0367	0.0252	0.0218
Mean Shear Force (x 10^3 kN)	15910.84	15482.57	12130.18	12360.66
Standard Deviation σ_F	3844.38	3693.26	2570.56	2218.88

Table 2 describes the comparison of maximum hysteresis energy exhibited by the isolated NPP under long and short-period ground motions of both the real and the simulated nature. The overall impact for each type of earthquake is studied by comparing mean and standard deviation values to get the upper and lower limit of the effect. The maximum hysteresis energy is clearly dissipated by the structure when subjected to ground motions with large long-period component. In case of real long and short-period seismic inputs, the 25 % higher mean values indicate the oppressive performance of the NPP under long-period ground motions. Whereas, the mean value difference turns to almost 32% while comparing the response under simulated long-period motions with that of short-period motion inputs. In addition, the overall mean hysteresis energy of NPP under simulated long-period motions is found slighty higher in magnitude than that of the energy value acquired by real long –period motions.

Table 2. Comparison of maximum hysteresis energy (KN.m).

Long-period			Short-period		
	Real	Simulated		Real	Simulated
Record Name	Max. Energy		Record Name	Max. Energy	
CHB009	20457.82	28023.3	MYGH06-NS	5146.25	6747.0
TKY005	14130.03	14471.1	AKT012-EW	11386.72	9254.7
TKY006	29772.95	27996.0	AOMH06-NS	28880.00	27083.4
TKY007	8705.60	14195.3	YMTH01-NS	16633.38	11810.0
TKY014	24911.28	23251.9	YMN002-EW	8804.48	9639.4
TKY015	18080.67	17403.6	YMT010-EW	15801.70	14379.9
TKY020	20203.73	13676.7	YMT010-NS	16002.98	15765.9
Mean	19466.01	19859.7	Mean	14667.64	13525.8
Mean - Std	12591.06	13408.1	Mean - Std	7091.58	6795.24
Mean + Std	26340.97	26311.3	Mean + Std	22243.70	20256.3

Figure 6 portrays the scenario to determine the mean hysteresis energy per cycle, dissipated by the NPP for each type of the ground motion. The mean energy curve initiates by slightly acquiring a rising trend with time but the change is pronounced more as the time ascends. The curve turns relatively steeper in the time range corresponding to 5~ 95% of maximum energy dissipated i.e. $E_{\max}$. Hence, the per cycle dissipated energy is determined by using the energy response data lying in the bounds of E_5 and E_{95} as shown in Figure 6.

The results are then compared in table 3 for better demonstration. For the long-period real ground motions, the mean hysteretic energy per cycle is 4.10% higher than that of long-period simulated ground motions. While, in case of short-period ground motions, the simulated ground motion has exhibited 4.84% greater response. Such deviations are acceptable as the relative error e_{rr} is kept under 10~15% while simulation and generation of the ground motions. Furthermore, in comparison to short-period real ground motions, 27.7% higher mean energy dissipation per cycle is augmented by the NPP under long-period real seismic motion. Whereas, for simulated earthquakes, the response deviates up to 20.72% if the comparative mean hysteretic energies resulted by long and short-period seismic inputs are observed.

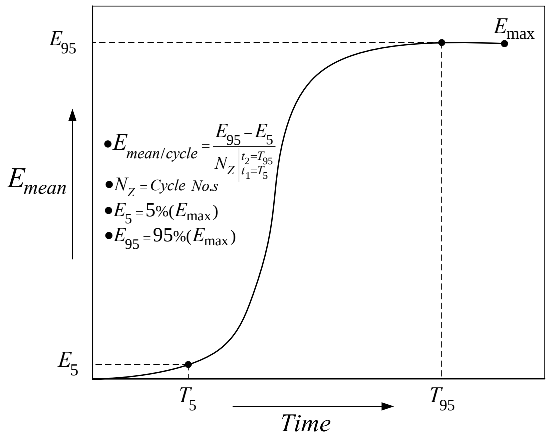

Figure 6. Mean hysteresis energy dissipated per cycle.

Table 3. Comparison of mean hysteresis energy per cycle (KN.m).

Ground Motion		E_5	T_5(sec)	E_{95}	T_{95}(sec)	N_Z	$E_{mean/cycle}$
Long-Period	Real	973.472	67.69	18495.96	194.04	94	186.4095
	Simulated	993.175	70.00	18870.33	192.94	100	178.7715
Short-Period	Real	733.49	39.93	13936.37	163.61	98	134.7233
	Simulated	676.39	32.63	12851.34	140.18	86	141.5692

5. CONCLUSIONS

Since, after the devastating event of Tohoku earthquake, the curiosity of setting the guidelines in the seismic design code of structures has been keenly observed. The high-rise buildings and structures with medium and long natural periods were badly manifested by the long-period wave component of this event. The generation and propagation of such onerous attribute of these earthquakes are more associated with the far-source ground motions rather than near-fault. Such long-period wave motions can act more severe if the structures are located in the area of deep soil plateau and high seismic hazards. Hence, based on such arguments, the present study reports the response of base-isolated NPP subjected to long-period ground motions. In order to encounter the uncertainties in the response, earthquakes are generated in accordance with real long and short-period seismic motions using ARMA model approach. The base isolated NPP is brought to act by both real and simulated excitations. The conclusions drawn from the study are as follows:

The generation and simulation of the seismic motions is done using ARMA model. The model provides an efficient approach to simulate the short-period earthquake motions by small number of parameters. Eventually, due to complex and lengthy time history, the high and low frequency component of long-period ground motions are separated using wavelet transform. Later, only the high frequency content of a ground motion is precisely simulated using the described process. The spectral compatibility of the real and simulated motions is made sure by governing the relative error e_{rr} lesser than threshold error e_t.

The performance of the base-isolated NPP subjected to real & simulated; long & short-period ground motions is investigated using probabilistic approach. The mean displacement attributed by the NPP under real long-period inputs is 0.1246 m which is fairly large than that under real short-period motions i.e. 0.0875 m. Similarly, the mean displacement for simulated long-period motion input motion is found higher than the short-period motion. Hence, the comparative displacement magnification or deviating percentile is 30% and 26% for real and simulated excitations respectively.

Moreover, in case of long-period motions, the standard deviation value has made the structure to exceed the allowable displacement limit which in turn signifies the substantial failure of the NPP.

The structural model has shown great difference in the shear force resistance for the two groups i.e. long and short- period, of ground motions. Generally, under long-period excitations, the response is high but immense change in the difference of the force along the height is observed. The mean deviation is 24% and 20.1% at the initially stages for real and simulated motions, respectively, which is gradually minified along the elevation and negligibly small at the top. In the similar manner, the mean hysteresis energy dissipated by the isolated NPP is 25% greater under real long-period ground motion whereas 32 % higher energy is dissipated in case of simulated long-periods motions. The scenario for calculating the mean hysteretic energy per cycle is explained. It is noticed that 27.7% higher energy dissipation is augmented by the NPP under long-period real seismic motion. But the response deviates up to 20.72% for simulated excitations.

Hence, under long-period ground motions the overall response of the base-isolated NPP is seen to be much amplified as compared to short-period ground motions .So, it can be inferred that such ground motions can cause magnified damages and hazards to the NPP in similar proportions. This fact necessitates the need to consider the effects of long-period components of earthquakes in the seismic design provisions of the safety related and high-rise structures with greater natural periods such as base-isolated NPP.

AKCNOWLEDGEMENT

This research was supported by the Ministry of Knowledge Economy and Korea Institute of Energy Technology Evaluation and Planning (KETEP) as a part of the Nuclear R&D. The authors would like to express their appreciation for the financial support.

REFERENCES

Ali, A., Dong, Y., Kim, D. and Cho, S.G. (2012). Dyanmic response of base isolated NPPs under long period seismic excitations. 9th International Conference on Urban Earthquake Engineering/ 4th Asia Conference on Earthquake Engineering, 1391-1396.

American Society of Civil Engineers (2010). Minimum Design Loads for Buildings and Other Structures, ASCE Standard (ASCE/SEI 7-10).

Araki, Y., Kim, M., Okayama, S., Ikago, K. and Uetani, K. (2011). Dynamic Instability in High-Rise SMRFs Subjected to Long-Period Ground Motions. *World Academy of Science, Engineering and Technology*, **59**, 2496-2503.

Dong, Y., Ji, S. and Xiao, M. (2004). Simulation of ground motions using time varying vector ARMA model. *13th World Conference on Earthquake Engineering*, Vancouver, Canada, 13WCEE.

Dong,Y. (2000). Application of ARMA Model for Simulation of Ground Motions and Spectra Estimation. (in Chinese) Thesis for master degree, Chongqing Jianzhu University, Chongqing.

Hurtado, J.E., Barbat, A.H. and DaChunha, A.A.M.F. (1996). Nonlinear random vibration of base isolated buildings under evolutionary seismic input. *11th World Conference on Earthquake Engineering*, Acapulco, Mexico, 11WCEE.

Lee, N.H., Song, K.B. (1999). Seismic capacity evaluation of the prestressed/reinforced concrete containment. Young-Gwang nuclear power plant units 5 & 6, *Nuclear Engineering and Design*, **192**, 189-203.

McKenna, F., Fenves, G.L. (2001). OpenSees, the open system for earthquake engineering simulation. http://opensees.berkeley.edu

Mobarakeh, A.A., Rofooei, F.R. and Ahamdi, G. (2002). Simulation of earthquake records using time-varying Arma (2, 1) model. *Probabilistic Engineering Mechanics*, **17**,15-34.

Naeim, F., Kelly, J.M. (1999) Design of seismic isolated structures: from theory to practice. *John Wiley and Sons, Inc.*, New York, USA.

Popescu,TH.D. and Demetriu, S. (1990). Analysis and simulation of strong earthquake ground motions using ARMA models. *Automatica*, **26:4**, 1990, 721-737.

Regulatory Guide 1.60. (1973). Design Response Spectra for Seismic Design of Nuclear Power Plants. *U.S. Nuclear Regulatory Commission*, Washington, DC.

Regulatory Guide 1.208. (2007). A Performance-Based Approach to Define the Site-Specific Earthquake Ground Motion. *U.S. Nuclear Regulatory Commission*, Washington, DC.

Takewaki, I. (2011). Preliminary report of the 2011 off the Pacific coast of Tohoku Earthquake. *J. Zhejiang Univ-Sci. A (Appl Phys & Eng)*, **12: 5**, 327-334.

Takewaki, I., Murakami, S., Fujita, K., Yoshitomi, S. and Tsuji, M. (2011). The 2011 off the Pacific coast of Tohoku earthquake and response of high-rise buildings under long-period ground motions. *Soil Dynamics and Earthquake Engineering*, **31**,1511-1528.

Xiang, Z. and Li, Yingmin. (2000). Statistical characteristics of long period response spectra of earthquake ground motion. *12th World Conference on Earthquake Engineering*, Auckland, New Zealand, 12WCEE, January.

Yang, P., Li, Y. M., Lai, M. (2000). A new method for selecting input waves for time history analysis. *China Civil Engineering Journal*, **33: 6**, 33-37.